Angewandte Zuschriften

Smart Materials

Deutsche Ausgabe: DOI: 10.1002/ange.201504153
Internationale Ausgabe: DOI: 10.1002/anie.201504153

Light- and Humidity-Induced Motion of an Acidochromic Film**

*Lidong Zhang and Panče Naumov**

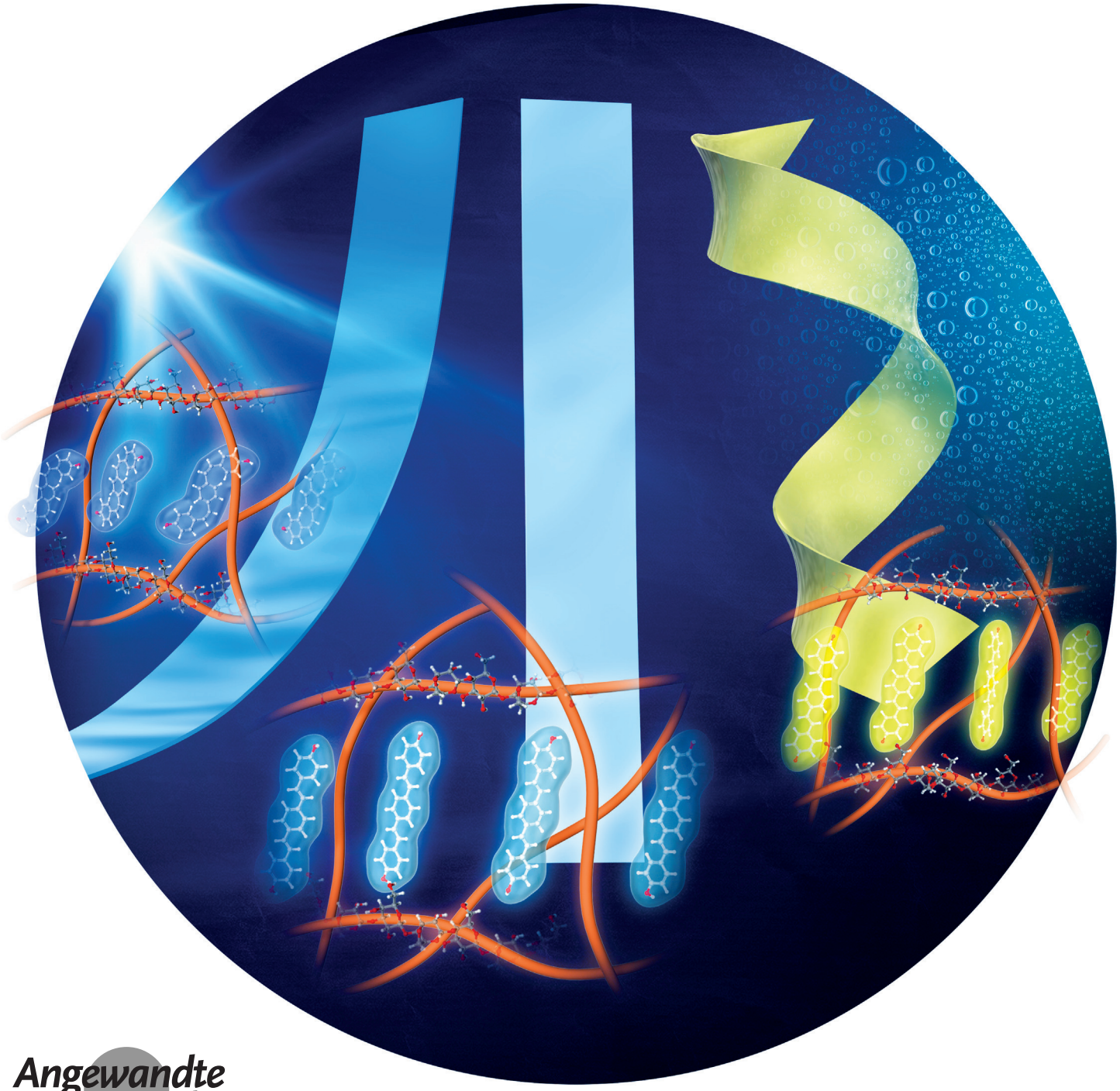

Abstract: *A smart acidochromic agarose-based film with 1,4-bis(para-hydroxystyryl)benzene as the pH-responsive fluorophore was prepared. This film can simultaneously harness the chemical potential of light and aerial humidity gradients to convert them into mechanical work. The strong reversible hygroscopicity of the agarose matrix induces swift locomotion by mechanical deformation owing to exchange of water with the surroundings. Driven by humidity, a 20 mg composite film coupled to a piezoelectric bending transducer sensor generates a peak output of approximately 80 mV, which corresponds to a power density of 25 $\mu W\,kg^{-1}$. Excitation with UV light triggers isomerization of the chromophore, which appears as reshaping by spiraling, bending, or twisting of the film. The material also responds to changes in the pH value by reversible protonation of the fluorophore with rapid changes in color and fluorescence. The threefold sensing capability of this smart material could be utilized for the fabrication of multiresponsive actuating dynamic elements in biomedicine and soft robotics.*

The rapid color variation displayed by some insects or animals, such as the amazing color changes of chameleons, is a natural phenomenon where the modulation of light absorption or reflection causes visual blending with the surroundings and secures the animal's survival. These impressive transformations are usually driven by chemical or morphological modifications of pigments in the cytoplasm that occur in response to external stimuli.[1–5] If applied to the design of artificial, biomimetic smart materials, the mechanistic principles of this phenomenon could contribute to specific applications that require optical camouflage, for instance within the context of security and defense.[6–9] Rapid changes in color (chromism) can be induced by changes in temperature, pressure, pH, or ionic strength, or by interaction with light.[10–19] Acidochromism, that is, pH-induced color modulation, is of importance in the design of pH sensors.[20–26] However, practical obstacles, such as difficulties with the handling and fabrication of macroscopic devices as well as safety concerns, limit the usefulness of liquid acidochromic materials. Embedding pH-responsive components into polymer matrices is a convenient approach to sensing materials that are devoid of fatigue and have reasonably short response times.[13,15,20–26]

A fast-forward strategy to high capacities in the rapid and reversible uptake of water could be the use of hydrogels as swelling matrices.[27,28] Here, the acidochromic fluorophore 1,4-bis(*para*-hydroxystyryl)benzene (BHSB) was incorporated into agarose (AG) as a biogenic hydrogel matrix with a strong propensity for water absorption. Anisotropic and reversible absorption and desorption of water by the hybrid material results in an impressive mechanical response. With a simple actuator, it is demonstrated that this smart hybrid is capable of converting the chemical potential stored within a humidity gradient into motion over a moist surface, which can be further converted into electricity. The material is also photoresponsive, strongly fluorescent, and acidochromic, thus providing multiple means for control over its optical, mechanical, and chemical properties.

The acidochromic guest (BHSB; Figure 1 A) was synthesized according to a variant of a previously published method.[29,30] BHSB undergoes a clear color change from colorless to yellow under white-light irradiation in response to changes in the pH value. The discoloration is due to changes in its electronic structure caused by deprotonation/protonation of the hydroxy groups.[29] By embedding BHSB into an agarose matrix in a one-pot process, a hybrid composite (BHSB@AG) that contains 1.0 % (w/w) BHSB was prepared (for details, see the Supporting Information). The composite

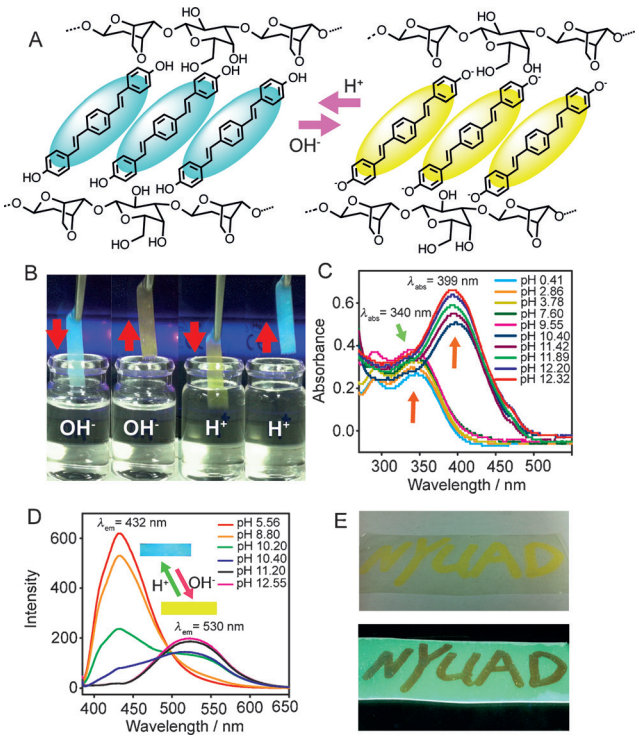

Figure 1. Structure and acidochromic response of a BHSB@AG hybrid film. A) The film responds to variations in pH value by protonation and deprotonation of BHSB. B) Reversible changes in fluorescence color induced by consecutive exposure of the film to acidic and alkaline aqueous solutions (SUV-4 UV lamp, $\lambda_{ex} = 254$ nm). C) UV/Vis spectral changes of the hybrid film that mirror the pH-dependent color change. The film was immersed in aqueous solutions of various pH values for 2 s before the spectra were recorded (moist film of pure agarose was used as a reference). D) Emission spectra of BHSB in MeOH/H_2O (2:1, v/v) at different pH values ($\lambda_{ex} = 373$ nm). E) Writing on the acidochromic film using alkaline solution (pH 10.40) as the ink. In the top and bottom images, the films were exposed to white light and UV light ($\lambda = 254$ nm), respectively.

[*] Dr. L. Zhang, Prof. P. Naumov
New York University Abu Dhabi
PO Box 129188, Abu Dhabi (United Arab Emirates)
E-mail: pance.naumov@nyu.edu

[**] We thank New York University Abu Dhabi for the financial support of this work and Dr. Nikolas Giakoumidis for his help with the design of the device for energy conversion. This research was partially carried out using Core Technology Platform resources at New York University Abu Dhabi.

Supporting information for this article is available on the WWW under http://dx.doi.org/10.1002/anie.201504153.

was cast onto pre-cleaned microscope slides and dried in air to prepare hybrid films of variable thicknesses.

Dry films of BHSB@AG were colorless and displayed strong blue fluorescence ($\lambda_{em} = 432$ nm; Figure 1B) when excited with weak UV light (ca. 3 $\mu W\,cm^{-2}$). When soaked in alkaline aqueous solution (pH 10.40), the hydroxy groups of BHSB were deprotonated, which led to an instantaneous change in the emission color from blue to yellow ($\lambda_{em} =$ 530 nm; Figure 1B,D, see also the Supporting Information, Movie S1).[29,31] The original blue fluorescence ($\lambda_{em} = 432$ nm) was restored by short immersion of the film in acidic solution (pH 1.10; Figure 1B) for fluorophore reprotonation. The emission color could be switched between yellow and blue many times without apparent distortion or damage; the film remained elastic, yet mechanically self-supporting. As shown in Figure 1E, the reversible acidochromism with a high contrast in the fluorescence of the two protonation states can be used for erasable writing (Movie S2). Using an alkaline aqueous solution (pH 10.40) as the ink, information can be written on a tablet made of the material. The text is readable with visible light or under UV light. Furthermore, the tablet is reusable, as the text can be erased by brief exposure to an acidic solution (pH 1.10).

Light has been employed as a convenient energy source to trigger photochemical or mechanical response.[32,33] BHSB embedded in an AG matrix can be used as a chromophore to harvest light and elicit a mechanical response. When slices of a thin film of BHSB@AG were exposed to UV light (20 $mW\,cm^{-2}$), they visibly deformed (Figure 2A–C). Depending on several factors, such as the aspect ratio (see below), the reshaping occurred as three kinematic effects:

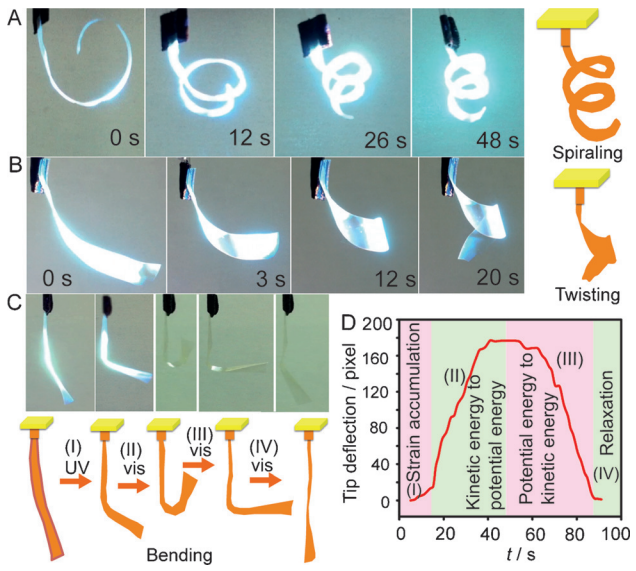

Figure 2. A–C) Kinematic analysis of the motility of a BHSB@AG hybrid film driven by UV light. Spiraling (A), twisting (B), and bending (C). "UV" and "vis" denominate exposure to ultraviolet and visible light, respectively. D) Typical trace of the film tip extracted from a video recording of its deflection. The film was exposed to light for 18 s, and maximal deflection was reached within 32 s. I–IV in panels C and D demarcate the four stages of bending in the process of light/kinetic/potential energy conversion performed by the film.

curling (Figure 2A; size: 6 cm × 3 mm × 40 μm), twisting (Figure 2B; 4 cm × 10 mm × 40 μm), and bending (Figure 2C; 4 cm × 0.5 mm × 40 μm). With continuous illumination, the spring-like ribbons formed within 48 s from the onset of excitation (Movie S3), and the twisted structure evolved within 20 s (Movie S4). With long strips, the films bent only slightly during exposure to UV light, but continued to bend even after the excitation had been stopped (Movie S5). This observation indicates that the mechanical response is not a direct consequence of the photoexcitation, but due to relaxation of the matrix following much faster photoexcitation/de-excitation processes of the chromophore. The mechanical reconfiguration of the film accommodates the latent strains that develop in the AG matrix in response to photoisomerization. To assess the eventual contribution of photothermal effects, a film of BHSB@AG was exposed to UV light (20 $mW\,cm^{-2}$), and the change in the surface temperature was recorded with an infrared thermographic camera. Upon irradiation with UV light, the temperature of the film increased by $< 6\,°C$, and did not exceed 33 °C (Figure S14 and Movie S10). In a second experiment, the same film was heated with a heated metal rod (Figure S14, Movie S11). The film did not bend even at a temperature of approximately 36 °C. This result confirmed that the bending of the film was induced by light and not by photothermal effects.

Closer inspection of the motion tracked by the deflection of the film tip (Figure 2D) revealed that a typical mechanical effect proceeded as a sequence of four stages (a detailed discussion of the kinematic analysis is provided in the Supporting Information): I) The film initially harvests the excitation energy; in this "light stage", the accumulation of strain determines the maximal degree of bending. II) After the excitation has been stopped, in the "dark stage", the film bends to relieve the strain by converting the accrued elastic energy into kinetic energy. During the bending, the kinetic energy is converted into potential energy, until the film reaches its maximal deflection. III) After the kinetic energy has been exhausted, the film starts to straighten whereby the potential energy is converted back into kinetic energy. IV) Finally, the film relaxes to restore its original shape, and its tip returns to the initial position. The thickness affects the rigidity of the strip and the spatial uniformity of photoconversion; therefore, it determines the maximal deflection and rate of bending. The responses from strips of various thicknesses (40, 60, and 100 μm) but identical lengths and widths are shown in Figure S13 and Movie S12. The thinnest strip bent the most, and the effect decreased with thicker strips. An increase in thickness improved the mechanical strength, but led to a decrease in the flexibility and the response to light.

In a series of experiments using different film strips, we could not detect any consistency in the directionality of the UV-induced spiraling, twisting, or bending. However, we noticed that each strip underwent only one kinematic effect (for instance, a strip that underwent spiraling did not twist or bend). This behavior indicates that the type of kinematic effect is determined by the orientation of the guest molecules in the matrix. To verify this hypothesis, several strips were cut

in different directions from the same film, and their motion was analyzed. They exhibited different responses, in line with the anisotropic distribution of the fluorophores in the matrix. We assume that this directionality is spontaneously acquired during the preparation of the film as a consequence of the prolate shape of the all-*trans* isomer of BHSB (Figure 1 A), although this hypothesis requires additional verification.

To further demonstrate the potential practical application of the mechanical response in biomimetic devices, we crafted a ribbon of BHSB@AG into a spring-like device (for details on the fabrication procedure, see the SI). When exposed to UV light, the ribbon visibly expanded to unwind (Figure 3 B, Movie S6). This motion visually resembles that observed with the coiling and overwinding of plant tendrils, which occurs by orthogonal shrinking and expansion of cell walls.[34] However, in the system described here, the strain anisotropy is achieved by photoinduced strains that are generated by isomerization at a molecular level rather than by changes in the cell turgor at a microscopic level (Figure 3 A).[34,35]

The *trans*-to-*cis* isomerization of BHSB was monitored by UV/Vis spectroscopy, by exposure of a dry film of BHSB@AG to UV light. Assuming similar molar absorption coefficients for the BHSB isomers, the absorption spectra in Figure 3 C indicate that before excitation with UV light, the BHSB moieties in the AG matrix exist mostly as the energetically most stable all-*trans* isomer, with a small contribution from the *cis–trans* isomer. The photoexcitation decreased the intensity of the all-*trans* band at approximately 330 nm with a simultaneous blue-shift and intensification of the *cis–trans* band at about 300 nm and evolution of a new band at approximately 260 nm. The variations of the concentrations of the three species (all-*trans*, all-*cis*, *cis–trans*) follow complex kinetics determined by two parallel processes, namely the direct conversion of the all-*trans* isomer into the all-*cis* isomer and indirect conversion via a *cis–trans* intermediate.[36–38] This behavior resembles that observed in solution (Figure 3 E); however, the isomerization is expectedly decelerated by steric constraints (Figure 3 C, E). To investigate the reversibility of the isomerization of BHSB, the all-*trans* form was initially converted into the all-*cis* form by exposure to UV light for ten minutes, which resulted in a blue-shift of the main absorption band to approximately $\lambda =$ 260 nm. The film was subsequently exposed to visible light ($\lambda > 400$ nm) to induce *cis*-to-*trans* isomerization. However, this process was very slow (Figure 3 D). We surmised that some of the BHSB molecules could form [2+2] photodimers in the matrix during UV irradiation. To verify this hypothesis, ^{1}H NMR spectra of BHSB@AG were recorded before and after UV irradiation for ten minutes. The spectrum after irradiation (Figure S11) did not contain new peaks between 3.5 and 5.5 ppm, which would be characteristic for the dimeric products. The increase in intensity of the peak at $\delta = 6.6$ ppm further supports the hypothesis that the *trans*-to-*cis* isomerization is induced by UV light. The absence of fatigue upon repeated cycling (Figure S12 and Movie S11) is in line with these conclusions.

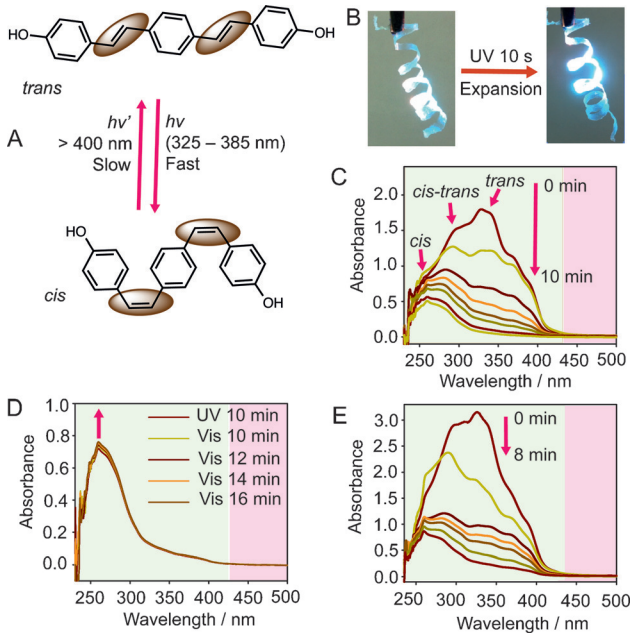

Figure 3. Mechanism of the mechanical response of the BHSB@AG film to excitation with UV light. A) Double *trans*-to-*cis* isomerization of BHSB moieties accounts for the anisotropic contraction of the fluorophore and causes a mechanical deformation of the film. B) Light-induced expansion of a spring-like strip of BHSB@AG mimicking the coiling of a plant tendril. C) Time-dependent UV/Vis spectra of the film recorded during continuous UV irradiation against pure AG as a reference. D) Evolution of the UV/Vis spectrum recorded after the film had been irradiated with UV light for 10 min ("UV") and then kept in visible light ("Vis"). E) Time-dependent UV/Vis spectra of BHSB irradiated with UV light in dimethylformamide.

Being composed of approximately 99 % hydrogel, the hybrid film BHSB@AG was expected to respond to environmental humidity by exchange of water with the surroundings. Indeed, when the film was placed on a paper that was pre-moistened with D_2O, it quickly curled up by swelling owing to the non-uniform absorption of D_2O. In the ATR-IR spectrum (for details, see the Supporting Information), the band at approximately 2500 cm^{-1}, which corresponds to the ν(OD) mode of D_2O absorbed by the film, was more intense for the lower than for the upper face of the film (Figure 4 A). This result indicates that water absorption is faster on the lower face of the film (which is in contact with water) than on the upper face. During this process, simultaneous water absorption and desorption occur between the film and the paper, which induces anisotropic swelling, whereby the film is quickly deformed. This dynamic D/H exchange between the D_2O-saturated film and the air is reflected in the IR spectra of the film that was saturated with D_2O (Figure 4 B). The decrease in the intensity of the band at 2500 cm^{-1} and evolution of the bands at 3400 cm^{-1} with time indicates continuous exchange of D_2O and HDO with aerial H_2O.

When the hybrid film was placed on a moist substrate, the uneven swelling of the two largest faces induced instantaneous curling (Figure 4 C). The rapid deformation induced mechanical instability, causing sliding and rolling, whereby the two opposite faces were alternatively and repeatedly brought into contact with the base. As a result, the film underwent a six-step kinematic process (I–VI in Figure 4 C) and dramatic locomotion, which appeared as self-actuated

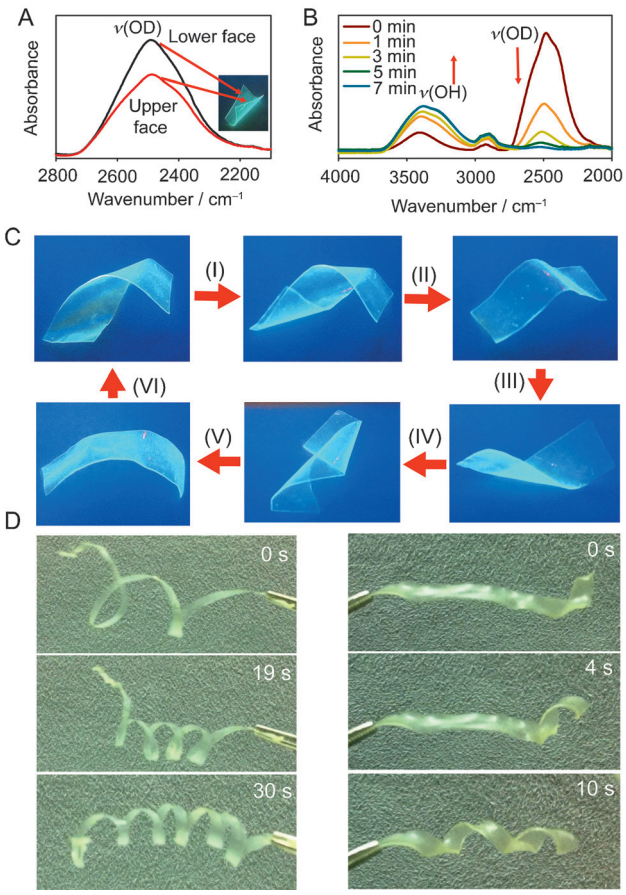

Figure 4. Mechanical motility of the hybrid film BHSB@AG in response to humidity. A) ATR-IR spectra of the film recorded after it had been placed on a paper saturated with D_2O (ca. 30% D_2O, w/w) for 10 s. B) ATR-IR spectra of a small piece of the film that was soaked in D_2O for 20 s (the excess D_2O on the surface was removed carefully using dry filter paper). The first spectrum ($t = 0$ min) was recorded immediately after the sample was removed from the paper. C) Locomotion of the film on a moist filter paper under irradiation with weak UV light (power density ca. 3 $\mu W cm^{-2}$, $\lambda = 254$ nm). D) Coiling of a film with helical shape and a thickness of 40 μm (left) or 200 μm (right) in response to a change in the humidity gradient.

creeping over the substrate (Movie S7). As opposite sides are exposed to different relative humidities, this dynamic element effectively converts the chemical potential of the humidity gradient into kinetic energy, which drives its motility. When exposed to a flow of humid air at approximately 35 °C, long strips of BHSB@AG rapidly coiled in a manner that resembles the coiling of cucumber tendrils, which bend and twist to find a support and lift the plant upwards (Figure 4D, Movies S8 and S9).[34] In line with our intuitive expectations, the coiling speed depended on the thickness of the film; thinner films were more flexible and coiled faster than thicker films (Figure 4D).

When the film was placed on a moist substrate in a sealed environment-controlled chamber at constant humidity, it only rolled up into a tubular shape and remained static (the curling is due to the contact with the moist surface). Thus, similar to another actuating material,[39,40] the motility of the film requires a gradient in humidity rather than a high relative humidity. To determine the effect of photoexcitation on motility as well as to better visualize the motion trajectory, the creeping film was exposed to very weak UV light (power density ca. 3 $\mu W cm^{-2}$, $\lambda = 254$ nm). The effect of UV irradiation on the deformation and motion of the film was negligible, and we were not able to detect any effects of light on its locomotion (Movie S7).

The perpetual deformation of the BHSB@AG film driven by exposure to non-uniform humidity could be utilized for transduction of the energy stored within the humidity gradient into mechanical energy, which can further be converted into electrical energy. As a demonstration of the capability of this material to generate electricity, the film was coupled with a bending sensor as a piezoelectric transducer, which converts the mechanical force into electrical power (Figure 5A). Subjecting this energy-harvesting device to humidity generates a bending moment in the BHSB@AG film that is transferred to the generator, causing an alternating current to pass through the resistor (Figure 5B–D).[39,41] When a 0.3 MΩ resistor was loaded onto a generator that included a 20 mg strip of BHSB@AG as the actuator, the peak output reached approximately 80 mV (Figure 5B). This device is capable of harvesting humidity to generate an average power output of approximately 0.5 nW and a power density of 25 $\mu W kg^{-1}$ (relative to the mass of the actuator). These values were significantly higher than the background (0.014 nW, Figure S10). It should be noted that the necessity to overcome the external force related to the stiffness of the generator inevitably alleviates the efficiency of the actuator in this experiment. Direct coupling of the composite with a piezoelectric material to design a monolithic actuator–generator conjugate should alleviate this energy dissipation. The results presented here highlight the potential of mechanically responsive smart hybrid materials for applications in biomedical devices, soft robotics, and energy harvesting.[34,42–46]

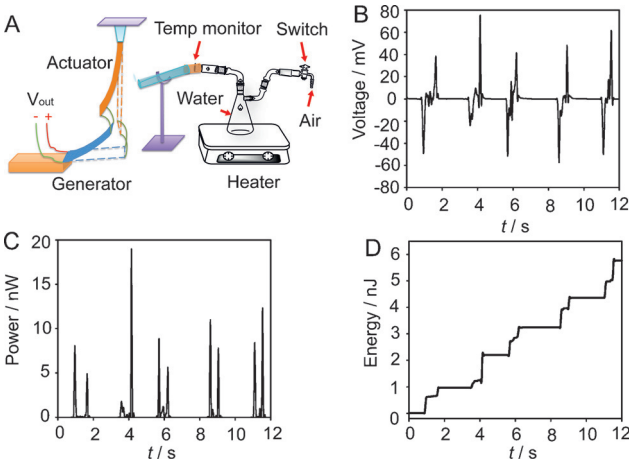

Figure 5. Harvesting of the energy of the humidity gradient to generate electricity. A) Schematic representation of the humidity-driven energy-harvesting device. As the moist air reaches the actuator, the bending moment is transferred to a piezoelectric transducer, where the mechanical energy is converted into electrical energy. B) Voltage generated across a 0.3 MΩ resistor. C) Instantaneous power and D) electrical energy delivered to the resistor.

Keywords: acidochromism · actuators · fluorescence · photochromism · smart materials

How to cite: *Angew. Chem. Int. Ed.* **2015**, *54*, 8642 – 8647
Angew. Chem. **2015**, *127*, 8766 – 8771

[1] S.-F. Devi, M. Adnan, *PLoS Biol.* **2008**, *6*, 22 – 29.
[2] J. P. Vigneron, J. M. Pasteels, D. M. Windsor, Z. Vértesy, M. Rassart, T. Seldrum, J. Dumont, O. Deparis, V. Lousse, L. P. Biró, D. Ertz, V. Welch, *Phys. Rev. E.* **2007**, *76*, 031907.
[3] R. E. Young, F. M. Mencher, *Science* **1980**, *208*, 1286 – 1288.
[4] W. J. Crookes, L.-L. Ding, Q. L. Huang, J. R. Kimbell, J. Horwitz, M. J. McFall-Ngai, *Science* **2004**, *303*, 235 – 238.
[5] A. R. Tao, D. G. DeMartini, M. Izumi, A. M. Sweeney, A. L. Holt, D. E. Morse, *Biomaterials* **2010**, *31*, 793 – 801.
[6] M. Kolle, P. M. Salgard-Cunha, M. R. J. Scherer, F. Huang, P. Vukusic, S. Mahajan, J. J. Baumberg, U. Steiner, *Nat. Nanotechnol.* **2010**, *5*, 511 – 515.
[7] J.-W. Oh, W.-J. Chung, K. Heo, H.-E. Jin, B. Lee, E. Wang, C. Zueger, W. Wong, J. Meyer, C. Kim, S.-Y. Lee, W.-G. Kim, M. Zemla, M. Auer, A. Hexemer, S.-W. Lee, *Nat. Commun.* **2014**, *5*, 3043.
[8] P. Vukusic, J. R. Sambles, *Nature* **2003**, *424*, 852 – 855.
[9] J. D. Forster, H. Noh, S. F. Liew, V. Saranathan, C. F. Schreck, L. Yang, J.-G. Park, R. O. Prum, S. G. J. Mochrie, C. S. O'Hern, H. Cao, E. R. Dufresne, *Adv. Mater.* **2010**, *22*, 2939 – 2944.
[10] J. H. Holtz, S. A. Asher, *Nature* **1997**, *389*, 829 – 832.
[11] C. Mao, A. Liu, B. Cao, *Angew. Chem. Int. Ed.* **2009**, *48*, 6790 – 6810; *Angew. Chem.* **2009**, *121*, 6922 – 6943.
[12] Q. Yang, S. Zhu, W. Peng, C. Yin, W. Wang, J. Gu, W. Zhang, J. Ma, T. Deng, C. Feng, D. Zhang, *ACS Nano* **2013**, *7*, 4911 – 4918.
[13] B. Chu, T. Qi, J. Liao, J. Peng, W. Li, S. Fu, F. Luo, Z. Qian, *Sens. Actuators B* **2012**, *166 – 167*, 56 – 60.
[14] M. D. Kim, S. A. Dergunov, E. Lindner, E. Pinkhassik, *Anal. Chem.* **2012**, *84*, 2695 – 2701.
[15] K. Ertekin, S. Alp, C. Karapire, B. Yenigül, E. Henden, S. Íçli, *J. Photochem. Photobiol. A* **2000**, *137*, 155 – 161.
[16] S. Inal, J. D. Kölsch, F. Sellrie, J. A. Schenk, E. Wischerhoff, A. Laschewsky, D. Neher, *J. Mater. Chem. B* **2013**, *1*, 6373 – 6381.
[17] J. Ma, Y. Li, T. White, A. Urbas, Q. Li, *Chem. Commun.* **2010**, *46*, 3463 – 3465.
[18] Y. Tao, Z. A. Dreger, Y. M. Gupta, *Vib. Spectrosc.* **2014**, *73*, 138 – 143.
[19] K. S. Sarkisyan, I. V. Yampolsky, K. M. Solntsev, S. A. Lukyanov, K. A. Lukyanov, A. S. Mishin, *Sci. Rep.* **2012**, *2*, 608.
[20] Z. Yang, W. Qin, J. W. Y. Lam, S. Chen, H. H. Y. Sung, I. D. Williams, B. Z. Tang, *Chem. Sci.* **2013**, *4*, 3725 – 3730.
[21] R. C. Somers, R. M. Lanning, P. T. Snee, A. B. Greytak, R. K. Jain, M. G. Bawendi, D. G. Nocera, *Chem. Sci.* **2012**, *3*, 2980 – 2985.
[22] P. Shi, Z. Liu, K. Dong, E. Ju, J. Ren, Y. Du, Z. Li, X. Qu, *Adv. Mater.* **2014**, *26*, 6635 – 6641.
[23] G. Li, S. Zhang, N. Wu, Y. Cheng, J. You, *Adv. Funct. Mater.* **2014**, *24*, 6204 – 6209.
[24] X. Zhang, S. Rehm, M. M. Safont-Sempere, F. Würthner, *Nat. Chem.* **2009**, *1*, 623 – 629.
[25] P. K. Ang, W. Chen, A. T. S. Wee, K. P. Loh, *J. Am. Chem. Soc.* **2008**, *130*, 14392 – 14393.
[26] T. Berbasova, M. Nosrati, C. Vasileiou, W. Wang, K. S. S. Lee, I. Yapici, J. H. Geiger, B. Borhan, *J. Am. Chem. Soc.* **2013**, *135*, 16111 – 16119.
[27] L. Zhang, Y.-I. Jeong, S. Zheng, S. I. Jang, H. Suh, D. H. Kang, I. Kim, *Polym. Chem.* **2013**, *4*, 1084 – 1094.
[28] L. Zhang, Y.-I. Jeong, S. Zheng, D. H. Kang, H. Suh, I. Kim, *Macromol. Biosci.* **2014**, *14*, 401 – 410.
[29] K. M. Solntsev, P. L. McGrier, C. J. Fahrni, L. M. Tolbert, U. H. F. Bunz, *Org. Lett.* **2008**, *10*, 2429 – 2432.
[30] J. Kunzelman, M. Kinami, B. R. Crenshaw, J. D. Protasiewicz, C. Weder, *Adv. Mater.* **2008**, *20*, 119 – 122.
[31] P. L. McGrier, K. M. Solntsev, A. J. Zucchero, O. R. Miranda, V. M. Rotello, L. M. Tolbert, U. H. F. Bunz, *Chem. Eur. J.* **2011**, *17*, 3112 – 3119.
[32] Y. Zhou, D. S. Wang, S. L. Huang, G. Auernhammer, Y. J. He, H. Butt, S. Wu, *Chem. Commun.* **2015**, *51*, 2725 – 2727.
[33] Z. Chen, S. Q. He, H. Butt, S. Wu, *Adv. Mater.* **2015**, *27*, 2203 – 2206.
[34] S. Iamsaard, S. J. Aßhoff, B. Matt, T. Kudernac, J. J. L. M. Cornelissen, S. P. Fletcher, N. Katsonis, *Nat. Chem.* **2014**, *6*, 229 – 235.
[35] S. J. Gerbode, J. R. Puzey, A. G. McCormick, L. Mahadevan, *Science* **2012**, *337*, 1087 – 1091.
[36] M. Ikegami, M. Nagao, H. Katayama, F. Ozawa, T. Arai, *Bull. Chem. Soc. Jpn.* **2007**, *80*, 1833 – 1835.
[37] H. Katayama, M. Nagao, F. Ozawa, M. Ikegami, T. Arai, *J. Org. Chem.* **2006**, *71*, 2699 – 2705.
[38] F. J. Lange, M. Leuze, M. Hanack, *J. Phys. Org. Chem.* **2001**, *14*, 474 – 480.
[39] M. Ma, L. Guo, D. G. Anderson, R. Langer, *Science* **2013**, *339*, 186 – 189.
[40] L. T. de Haan, J. M. N. Verjans, D. J. Broer, C. W. M. Bastiaansen, A. P. H. J. Schenning, *J. Am. Chem. Soc.* **2014**, *136*, 10585 – 10588.
[41] X. Chen, L. Mahadevan, A. Driks, O. Sahin, *Nat. Nanotechnol.* **2014**, *9*, 137 – 141.
[42] M. A. C. Stuart, W. T. S. Huck, J. Genzer, M. Müller, C. Ober, M. Stamm, G. B. Sukhorukov, I. Szleifer, V. V. Tsukruk, M. Urban, F. Winnik, S. Zauscher, I. Luzinov, S. Minko, *Nat. Mater.* **2010**, *9*, 101 – 113.
[43] M. R. Islam, X. Li, K. Smyth, M. J. Serpe, *Angew. Chem. Int. Ed.* **2013**, *52*, 10330 – 10333; *Angew. Chem.* **2013**, *125*, 10520 – 10523.
[44] J. Q. Zhao, Y. Y. Liu, Y. L. Yu, *J. Mater. Chem. C* **2014**, *2*, 10262 – 10267.
[45] J. I. Mamiya, A. Kuriyama, N. Yokota, M. Yamada, T. Ikeda, *Chem. Eur. J.* **2015**, *21*, 3174 – 3177.
[46] R. Penterman, S. I. Klink, H. D. Koning, G. Nisato, D. J. Broer, *Nature* **2002**, *417*, 55 – 58.

Received: May 6, 2015
Published online: June 25, 2015

